9-18-2006

Short GRB and Binary Black Hole Standard Sirens as a Probe of Dark Energy

Neal Dalal
University of Toronto

Daniel E. Holz
Los Alamos National Laboratory; University of Chicago

Scott A. Hughes
Massachusetts Institute of Technology

Bhuvnesh Jain
University of Pennsylvania, bjain@physics.upenn.edu

http://dx.doi.org/10.1103/PhysRevD.74.063006

Short GRB and Binary Black Hole Standard Sirens as a Probe of Dark Energy

Abstract
Observations of the gravitational radiation from well-localized, inspiraling compact-object binaries can measure absolute source distances with high accuracy. When coupled with an independent determination of redshift through an electromagnetic counterpart, these standard sirens can provide an excellent probe of the expansion history of the Universe and the dark energy. Short γ-ray bursts, if produced by merging neutron star binaries, would be standard sirens *with known redshifts* detectable by ground-based gravitational wave (GW) networks such as Advanced Laser Interferometer Gravitational-wave Observatory (LIGO), Virgo, and Australian International Gravitational Observatory (AIGO). Depending upon the collimation of these GRBs, the measurement of about 10 GW-GRB events (corresponding to about 1 yr of observation with an advanced GW detector network and an all-sky GRB monitor) can measure the Hubble constant h to ~ 2–3%. When combined with measurement of the absolute distance to the last scattering surface of the cosmic microwave background, this determines the dark energy equation of state parameter w to ~9%. Similarly, supermassive binary black hole inspirals will be standard sirens detectable by Laser Interferometer Space Antenna (LISA). Depending upon the precise redshift distribution, ~100 sources could measure w at the ~4% level.

Disciplines
Physical Sciences and Mathematics | Physics

Comments
Suggested Citation:
Dalal, N., Holz, D.E., Hughes, S.A., and Jain, B. (2006). Short GRB and binary black hole standard sirens as a probe of dark energy. *Physical Review D*, 063006.

http://dx.doi.org/10.1103/PhysRevD.74.063006

Short GRB and binary black hole standard sirens as a probe of dark energy

Neal Dalal,[1] Daniel E. Holz,[2,3] Scott A. Hughes,[4] and Bhuvnesh Jain[5]

[1]*CITA, University of Toronto, 60 St. George St., Toronto, ON, M5S 3H8, Canada*
[2]*Theoretical Division, Los Alamos National Laboratory, Los Alamos, New Mexico 87545, USA*
[3]*Department of Astronomy and Astrophysics, University of Chicago, Chicago, Illinois 60637, USA*
[4]*Dept. of Physics and MIT Kavli Institute, 77 Massachusetts Avenue, Cambridge, Massachusetts 02139, USA*
[5]*Dept. of Physics and Astronomy, University of Pennsylvania, Philadelphia, Pennsylvania 19104, USA*

(Received 16 January 2006; published 18 September 2006)

Observations of the gravitational radiation from well-localized, inspiraling compact-object binaries can measure absolute source distances with high accuracy. When coupled with an independent determination of redshift through an electromagnetic counterpart, these standard sirens can provide an excellent probe of the expansion history of the Universe and the dark energy. Short γ-ray bursts, if produced by merging neutron star binaries, would be standard sirens *with known redshifts* detectable by ground-based gravitational wave (GW) networks such as Advanced Laser Interferometer Gravitational-wave Observatory (LIGO), Virgo, and Australian International Gravitational Observatory (AIGO). Depending upon the collimation of these GRBs, the measurement of about 10 GW-GRB events (corresponding to about 1 yr of observation with an advanced GW detector network and an all-sky GRB monitor) can measure the Hubble constant h to $\sim$2–3%. When combined with measurement of the absolute distance to the last scattering surface of the cosmic microwave background, this determines the dark energy equation of state parameter w to $\sim$9%. Similarly, supermassive binary black hole inspirals will be standard sirens detectable by Laser Interferometer Space Antenna *(LISA)*. Depending upon the precise redshift distribution, $\sim$100 sources could measure w at the $\sim$4% level.

DOI: 10.1103/PhysRevD.74.063006 PACS numbers: 04.30.Db, 95.36.+x, 98.70.Rz, 98.80.−k

I. INTRODUCTION

With the advent of the Laser Interferometer Gravitational-wave Observatory (LIGO), we are on the verge of an era of gravitational-wave (GW) astronomy [1,2]. Among the most interesting expected sources for GW observatories are compact-object binaries. Advanced LIGO, a planned upgrade with tenfold increase in sensitivity, would detect the inspirals and coalescence of stellar-mass binaries within several hundred megaparsecs, while the Laser Interferometer Space Antenna (*LISA*) would study supermassive binary black holes (SMBBH) ($M \sim 10^4$–$10^7 M_\odot$) throughout the universe ($z \lesssim 10$).

The idea of using GW measurements of coalescing binaries to make cosmologically interesting measurements has a long history. As originally pointed out by Schutz [3], observation of the gravitational radiation from an inspiraling binary provides a self-calibrated absolute distance determination to the source. Chernoff [4] and Finn [5] took advantage of this property to show that, by observing many inspiral sources, one can construct the distribution of observed binary mass and GW signal strength, and thereby statistically constrain the values of cosmological parameters. More recently, Holz and Hughes [6] have shown that *LISA* observations of well-localized SMBBH inspirals allow cosmological distance determination with unprecedented accuracy, with typical errors $<1\%$. These GW ''standard sirens'' can precisely map out the expansion history of the Universe, offering a powerful probe of the dark energy.

The utility of standard sirens for constraining dark energy is quite similar to that of standard candles, such as Type-Ia supernovae. One advantage of GW standard sirens is that the underlying physics is well-understood. The radiation emitted during the inspiral phase (as opposed to the merger phase) is well-described using the post-Newtonian expansion of general relativity [7]. An unknown systematic evolution of the standard sirens over time, precisely mimicking a different cosmology, is unlikely to be of concern. Furthermore, GW observatories directly measure absolutely calibrated source distances, whereas Type-Ia supernova standard candles provide only relatively calibrated distances.

A major drawback of GW standard sirens is that, although the gravitational waveforms measure distance directly, they contain no redshift information. To be useful as a standard candle, an independent measure of the redshift to the source is crucial. This can be determined through observation of an electromagnetic counterpart, such as the host galaxy of the source. Unfortunately, as GW observatories are essentially all-sky, they generally provide poor source localization, and the host galaxy is not always unambiguously identifiable [8]. In cases where source redshifts cannot be determined, the distribution of unlocalized events can be used to place statistical bounds on cosmological parameters [5]. In this paper we will focus on GW sirens with counterparts with measurable redshifts, as they can provide very tight constraints on cosmology.

Because standard siren distances are absolutely calibrated, even sources at low redshift (e.g., $z \lesssim 0.2$) can

constrain dark energy. This may seem surprising, since at low redshifts the distance-redshift relation is well-described by a linear Hubble relation $D = cz/H_0$, independent of dark energy parameters. As emphasized by Hu and Jain [9], and Hu [10], however, absolute distances to sources at low redshift tightly constrain dark energy, when combined with a determination of the absolute distance to the last-scattering surface of the cosmic microwave background (CMB). To understand this, note that cosmological distances are given by a redshift integral of the Hubble parameter, which in turn depends on the sum of energy densities at each redshift:

$$D(z_s) = \frac{c}{H_0\sqrt{\Omega_K}} \sinh\left[\sqrt{\Omega_K}\int_0^{z_s}\frac{H_0}{H(z)}dz\right]$$
$$\frac{H(z)}{H_0} = \sqrt{\Omega_m(1+z)^3 + \Omega_{\rm de}(1+z)^{3(1+w)} + \Omega_K(1+z)^2}. \quad (1)$$

Here $\Omega_m + \Omega_{\rm de} + \Omega_K = 1$, $H_0 = 100h$ km/s/Mpc is the Hubble constant today, and we have assumed a constant equation of state parameter, w. If we assume a flat universe ($\Omega_K = 0$), then $\Omega_{\rm de} = 1 - \Omega_m$, and the only parameters describing the global expansion are h, Ω_m, and w. Observations of the primary anisotropies in the CMB provide two constraints on these three parameters. First, the heights of the acoustic peaks determine the matter density (in g/cm^3), which fixes $\Omega_m h^2$. Second, the angular scale of the peaks (their location in l-space) precisely measures the angular diameter distance to the CMB last-scattering surface, in Mpc. Absolute distances to low-redshift sources measure the Hubble constant h, which then allows all three parameters to be determined [9,10]. The constraints we present would be substantially degraded if the curvature were not fixed to zero; see [11,12] for the prospects for precise constraints on curvature.

In addition to low-redshift standard sirens, those at higher redshifts also help constrain dark energy, in the same manner as high-redshift standard candles. Holz and Hughes [6] discuss how *LISA* observations of SMBBH inspirals can help constrain cosmology. For a dark energy model which is not dramatically different from a cosmological constant Λ, the interesting redshift range is when the dark energy density is significant ($z \lesssim 1$), although note that gravitational lensing degrades the constraints from the highest redshift standard sirens (or candles) [13].

As mentioned above, the GWs from standard sirens measure source distances, but do not measure source redshifts. An electromagnetic counterpart associated with the merger event will generally be required to use GW sources to determine cosmology. One potential class of GW sources guaranteed to have electromagnetic counterparts are short γ-ray bursts (GRBs). Some fraction of short GRBs are thought to arise in the mergers of neutron star (NS) binaries, and hence should be strong GW emitters in the frequency band accessible to ground-based observatories. The GRB counterpart to these GW source provides a precise sky localization, which is useful both for determining the redshift to the source, and for significantly improving the GW determination of absolute distance. As we discuss below, short GRBs occur at a rate large enough for them to provide interesting cosmological constraints.

II. DISTANCE DETERMINATION FOR INSPIRALING BINARIES

In this section we briefly review how distances to inspiraling binaries may be determined; see Ref. [14] for more detail. An inspiraling binary at direction $\hat{\boldsymbol{n}}$ on the sky, with orbital angular momentum axis $\hat{\boldsymbol{L}}$, generates GWs with strain tensor

$$\mathbf{h}(t) = h_+(t)\mathbf{e}^+ + h_\times(t)\mathbf{e}^\times, \quad (2)$$

where the basis tensors are

$$\mathbf{e}^+ = \boldsymbol{e}_x \otimes \boldsymbol{e}_x - \boldsymbol{e}_y \otimes \boldsymbol{e}_y \quad (3)$$

$$\mathbf{e}^\times = \boldsymbol{e}_x \otimes \boldsymbol{e}_y + \boldsymbol{e}_y \otimes \boldsymbol{e}_x \quad (4)$$

with

$$\boldsymbol{e}_x = \frac{\hat{\boldsymbol{n}} \times \hat{\boldsymbol{L}}}{|\hat{\boldsymbol{n}} \times \hat{\boldsymbol{L}}|} \quad (5)$$

$$\boldsymbol{e}_y = \boldsymbol{e}_x \times \hat{\boldsymbol{n}}. \quad (6)$$

Our convention is that $\hat{\boldsymbol{n}}$ points towards the source, hence the waves propagate in the direction $-\hat{\boldsymbol{n}}$. We express the amplitudes of the two polarizations $h_+(t)$ and $h_\times(t)$ in the frequency domain as

$$\tilde{h}_+(f) = (1+\upsilon^2)\tilde{h}_0(f), \qquad \tilde{h}_\times(f) = -2i\upsilon\tilde{h}_0(f) \quad (7)$$

where $\upsilon \equiv \hat{\boldsymbol{n}} \cdot \hat{\boldsymbol{L}}$ is the cosine of the inclination angle of the binary, and

$$\tilde{h}_0(f) = \sqrt{\frac{5}{96}}\pi^{-2/3}\left[\frac{G\mathcal{M}}{c^3}\right]^{5/6}\frac{c}{D}f^{-7/6}\exp[i\Psi(f)]. \quad (8)$$

In this expression, D is the luminosity distance to the source, and $\mathcal{M} = (1+z)[m_1m_2]^{3/5}/(m_1+m_2)^{1/5}$ is the redshifted chirp mass of the binary. The phase Ψ is given by

$$\Psi(f) = 2\pi f t_c - \phi_c - \frac{\pi}{4} + \frac{3}{4}\left(\frac{8\pi G\mathcal{M}f}{c^3}\right)^{-5/3}, \quad (9)$$

where t_c is the time at coalescence, and ϕ_c is the orbital phase at coalescence.

These expressions describe a binary's waves only in the Newtonian, quadrupole approximation—treating the binary's kinematics as due to Newtonian gravity and using the quadrupole formula to estimate its GW emission. Because the phase parameters are essentially uncorrelated from the

amplitude parameters, this approximation is good enough to estimate the expected signal-to-noise ratio (SNR) from a source, and provides a good estimate of the distance measurement accuracy, but is not accurate enough to reliably model the detailed GW waveform [14]. Higher order post-Newtonian templates (see Ref. [7] for detailed discussion) should be sufficiently accurate, and are used for the actual data analysis.

Given $\mathbf{h}(t)$, the measured strain is given by

$$h_M(t) = h^{ab}(t) d_{ab}, \tag{10}$$

where the detector response tensor for an interferometer with arms $\hat{\boldsymbol{l}}$ and $\hat{\boldsymbol{m}}$ is $\mathbf{d} = (\hat{\boldsymbol{l}} \otimes \hat{\boldsymbol{l}} - \hat{\boldsymbol{m}} \otimes \hat{\boldsymbol{m}})/2$. In the notation of Ref. [14], a detector at colatitude θ and longitude ϕ with orientation α has response tensor

$$\begin{aligned}\mathbf{d} = &\cos(2\alpha)[\boldsymbol{e}_\theta \otimes \boldsymbol{e}_\phi + \boldsymbol{e}_\phi \otimes \boldsymbol{e}_\theta]/2 \\ &- \sin(2\alpha)[\boldsymbol{e}_\theta \otimes \boldsymbol{e}_\theta - \boldsymbol{e}_\phi \otimes \boldsymbol{e}_\phi]/2.\end{aligned} \tag{11}$$

To recap, the source parameters determining the measured signal are distance D, chirp mass $\mathcal{M}$, coalescence time t_c, coalescence phase ϕ_c, source direction $\hat{\boldsymbol{n}}$, and orbital axis $\hat{\boldsymbol{L}}$. These are the 8 parameters to be determined from the data timestream $h_M(t)$. If the detector has strain noise with spectral density $S_h(f)$, then the incident strain is measured with SNR (assuming Wiener filtering):

$$\mathrm{SNR}^2 = 4 \int \frac{|\tilde{h}_M(f)|^2}{S_h(f)} df. \tag{12}$$

The complicated angular dependence is hidden within the measured strain $\tilde{h}_M$. This dependence can be made more explicit by rewriting the above equation as [5]

$$\mathrm{SNR}^2 = 4 \frac{\mathcal{A}^2}{D^2} [F_+^2 (1 + \upsilon^2)^2 + 4 F_\times^2 \upsilon^2] I_7, \tag{13}$$

where $\mathcal{A} = \sqrt{5/96}\pi^{-2/3}(G\mathcal{M}/c^3)^{5/6}c$, $F_+ = \mathbf{e}^+_{ab} d^{ab}$, $F_\times = \mathbf{e}^\times_{ab} d^{ab}$, and

$$I_7 = \int_{f_{\mathrm{low}}}^{\infty} \frac{f^{-7/3}}{S_h(f)} df. \tag{14}$$

Here $f_{\mathrm{low}} \simeq 10$ Hz is the frequency below which the detectors' sensitivities are badly degraded by ground motions. In the optimal case, the binary is face-on ($\upsilon = 1$) and directly overhead, so that $F_+^2 + F_\times^2 = 1$. This gives

$$\mathrm{SNR}_{\mathrm{opt}} = 4 \frac{\mathcal{A}}{D} I_7^{1/2}. \tag{15}$$

If instead we average over all-sky positions and binary orientations, we find

$$\mathrm{SNR}_{\mathrm{ave}} = \frac{8}{5} \frac{\mathcal{A}}{D} I_7^{1/2}, \tag{16}$$

where we have made use of $\langle F_+^2 \rangle = \langle F_\times^2 \rangle = 1/5$ and

$$\frac{1}{2} \int_{-1}^{1} (1 + \upsilon^2)^2 d\upsilon = \frac{28}{15} \tag{17}$$

$$\frac{1}{2} \int_{-1}^{1} 4\upsilon^2 d\upsilon = \frac{4}{3}. \tag{18}$$

Note that the SNR in the optimal geometry is a factor $5/2$ times larger than that for the average geometry. Also note that face-on sources, when averaged over all-sky positions, have SNR a factor $\sqrt{5/4} \simeq 1.12$ larger than $\mathrm{SNR}_{\mathrm{ave}}$.

We can estimate how well the parameters $\boldsymbol{p}$ are measured using the Fisher matrix

$$F_{ij} = 4 \int \mathrm{Re}\left[\frac{\partial_i \tilde{h}_M^*(f) \partial_j \tilde{h}_M(f)}{S_h(f)}\right] df, \tag{19}$$

where $\partial_i \equiv \partial/\partial p_i$, and $*$ denotes complex conjugation. Approximating the likelihood as

$$\mathcal{L} = \sqrt{\frac{|\mathbf{F}|}{(2\pi)^{n_p}}} \exp\left(-\frac{1}{2} \Delta \boldsymbol{p} \cdot \mathbf{F} \cdot \Delta \boldsymbol{p}\right), \tag{20}$$

then the error on parameter p_i is given by $\sqrt{(\mathbf{F}^{-1})_{ii}}$. Prior constraints, or constraints from multiple detectors, are implemented by multiplying the respective likelihoods, which in this approximation reduces to summing the respective Fisher matrices. In our calculations we compute the partial derivatives numerically by finite differencing. We note here that some (presently unquantified) error is introduced into our analysis by using Fisher matrices, which are strictly accurate only when the Gaussian approximation to the likelihood function is appropriate (the "high SNR" limit [14,15]). We are presently examining how parameter estimation (and thus our conclusions) are affected by directly computing the likelihood function, rather than working strictly within the Gaussian approximation.

In practice, the "phase" parameters $\mathcal{M}$, t_c, and ϕ_c are determined with exquisite precision. The "amplitude" parameters D, $\hat{\boldsymbol{L}}$, and $\hat{\boldsymbol{n}}$ are determined less well, in large part due to parameter degeneracies. By using multiple detectors many of these degeneracies can be broken. For example, timing information from a network of detectors helps determine the source direction $\hat{\boldsymbol{n}}$. Similarly, if the detectors have different response tensors $\mathbf{d}$, then the polarization of the GW signal may be measured, which constrains the orbital axis $\hat{\boldsymbol{L}}$ [c.f. Eq. (7)].

III. GRBS OBSERVED BY GW NETWORKS

Short GRBs are an extremely promising source of GWs. These sources have been of great interest recently, due to the prompt localization of the events by the *Swift*[1] [16,17] and *HETE-2*[2] [18] satellites, allowing their detection in X-

[1] http://swift.gsfc.nasa.gov/docs/swift/swiftsc.html
[2] http://space.mit.edu/HETE/Welcome.html

ray, optical, and radio frequencies. Particularly exciting has been the identification of several galaxies hosting short bursts [16,18,19]. While the nature of short GRBs is not yet known, a leading candidate is the merger of NS binaries [20], although other models have been proposed as well [21]. The detection or nondetection of GRBs in GWs would be extremely useful [22], for example, in confirming or refuting the NS-NS merger scenario, or determining the extent of collimation of the γ-ray emission [23].

Additionally, as mentioned above, short GRBs can also be very useful for determining the background cosmology by acting as GW standard sirens. One immediate advantage offered by GRBs is that their bright electromagnetic emission allows a precise localization of the source on the sky, pinpointing the source direction $\hat{\boldsymbol{n}}$ and lifting some of the degeneracies which limit distance determination. The extent of collimation in short GRBs is not well known, although recent analyses suggest that there may be a rather wide range in jet collimation from burst to burst [24,25]. For bursts that arise from binary NS mergers, our theoretical expectation is that emission should be beamed preferentially along the orbital angular momentum axis, where baryon loading is minimized. If this is the case, then we expect short GRBs to be nearly face-on, $\upsilon = \hat{\boldsymbol{n}} \cdot \hat{\boldsymbol{L}} \approx 1$. As can be seen from Eq. (7), this maximizes the amplitudes of both GW polarizations, and hence maximizes the SNR of the GW detection for a given source direction $\hat{\boldsymbol{n}}$. In what follows we compute distance errors for two cases: (1) isotropic distribution of $\hat{\boldsymbol{L}}$, and (2) collimation, assuming an inclination probability distribution $dP/d\upsilon \propto \exp(-(1-\upsilon)^2/2\sigma_\upsilon^2)$ for $\sigma_\upsilon = 0.05$, corresponding to a roughly 20° jet angle.

The expected chirp mass for GRBs, $\mathcal{M} \approx 1.2 M_\odot$, places them favorably in the frequency band accessible to ground-based GW observatories. Several such observatories are now operating or are planned for construction in the near future. LIGO is already operational, and its sensitivity should increase by an order of magnitude in a planned upgrade (Advanced LIGO) [26]. A detector of similar scale, Virgo [27], is under construction in Italy, and there are plans for a similar detector, AIGO [28], in Australia. The locations and orientations of these observatories are listed in Table I. The two LIGO detectors are oriented to have very similar response tensors, and therefore have limited ability to independently measure polarization (and hence inclination). In the absence of a strong, reliable prior, determining $\hat{\boldsymbol{L}}$ will thus require combining LIGO with other observatories.

TABLE I. Coordinates of GW observatories, in the notation of Ref. [14]. All values are in degrees.

Site	θ	ϕ	α
LIGO (Hanford)	43.54	−119.4	171
LIGO (Livingston)	59.44	−90.77	243
Virgo	46.37	10.5	115.6
AIGO	121.4	115.7	45

Henceforth we assume that all four detectors will observe GRB events; in subsequent work, we will investigate how the distance errors degrade if one or more elements of this network are removed. Preliminary results indicate that reducing the size of the detector network does not substantially degrade our ability to determine distance (aside from the loss in total SNR) *assuming that we can set a prior on the beaming factor* (and hence on the inclination angle). If we cannot set such a prior, then losing sites in this network badly degrades our ability to determine distance to these sources. We emphasize this point to highlight the importance of modeling bursts, and the importance of having widely separated GW detectors around the globe.

Figure 1 plots the noise spectral density forecasted for Advanced LIGO [26]. Projected noise curves for the advanced detector configurations are not yet available for Virgo or AIGO, so for simplicity we use the Advanced LIGO curve for all the observatories in the network. For comparison, we also show the sensitivity for the currently operating LIGO observatories.

With the response tensors for the elements in our network, and their noise spectra, we can now compute the Fisher matrices and parameter errors for GRBs as a function of distance and location on the sky. For convenience, when computing the Fisher matrix we replace the parameter pair $\{D, \upsilon = \hat{\boldsymbol{n}} \cdot \hat{\boldsymbol{L}}\}$ with the pair $\{(1+\upsilon)^2/D, (1-\upsilon)^2/D\}$, to avoid singularities in the limit $\upsilon \to 1$ when υ and D become degenerate [14]. Another difficulty that arises in the face-on limit is that the position angle of $\hat{\boldsymbol{L}}$, denoted ψ by Ref. [14], becomes meaningless as $\upsilon \to 1$. Including it as a parameter would cause the Fisher matrix to become singular in the face-on limit; we circumvent this difficulty using singular value decomposition to invert the

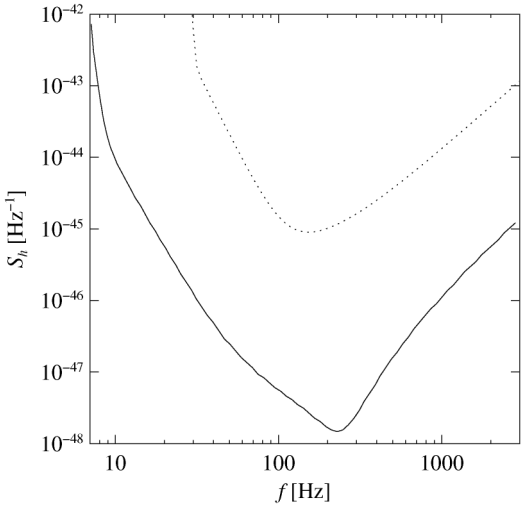

FIG. 1. Noise curve for the LIGO detectors, for initial (dotted) and advanced (solid) sensitivity.

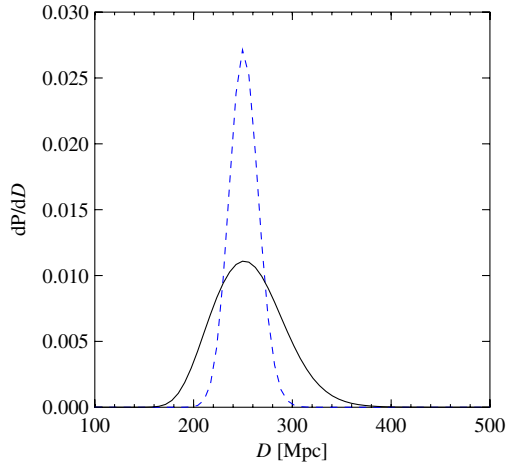

FIG. 2 (color online). Distribution of measured distances for a source at $D = 250$ Mpc, averaged over 100 source directions $\hat{\boldsymbol{n}}$ and orientations $\hat{\boldsymbol{L}}$. The solid curve shows constraints for randomly oriented sources, while the dashed curve shows constraints for collimated sources with $\sigma_\upsilon = 0.05$.

Fisher matrix, zeroing any eigenvalue whose magnitude is 10^{-10} times that of the largest eigenvalue.

Because the antenna response of each detector varies strongly with source direction $\hat{\boldsymbol{n}}$, the parameter errors at any given distance D also depend strongly on $\hat{\boldsymbol{n}}$. We are interested in average errors as a function of D; hence, for each D we average over 100 different orientations of $\hat{\boldsymbol{L}}$ and $\hat{\boldsymbol{n}}$. For example, Fig. 2 shows the expected constraints for sources at a distance of $D = 250$ Mpc. Note that the errors significantly improve if it is assumed that sources are beamed towards us.

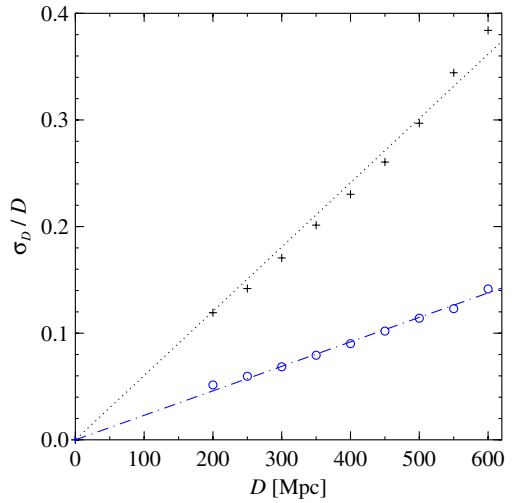

FIG. 3 (color online). Fractional distance errors as a function of source distance D. The + symbols are for unbeamed GRBs, while circles are for $\sigma_\upsilon = 0.05$. The two lines show the best-fit linear relations (see text); note that there may be departures from linear scaling at the highest distances.

Given the likelihood distribution dP/dD, we define the distance error as $\sigma_D^2 = \langle D^2\rangle - \langle D\rangle^2$, where averages are with respect to dP/dD. Figure 3 plots σ_D as a function of D. Our results appear roughly consistent with $\sigma_D/D \propto D \propto 1/\mathrm{SNR}$. Our best-fit linear scaling for unbeamed GRBs is $\sigma_D/D = D/(1.7\ \mathrm{Gpc})$, and $\sigma_D/D = D/(4.4\ \mathrm{Gpc})$ for collimation $\sigma_\upsilon = 0.05$. Henceforth we assume these scalings when estimating cosmological constraints from GW network observations of short GRBs.

IV. COSMOLOGICAL CONSTRAINTS FROM STANDARD SIRENS

As discussed in § I, a measurement of the Hubble constant h using GRB standard sirens, when combined with CMB constraints, enables constraints on dark energy parameters. We use two measurements from the CMB: determination of the angular scale of the acoustic peaks, l_A, and determination of the matter density, $\Omega_m h^2$, from the peak heights. Currently the Wilkinson Microwave Anisotropy Probe satellite has measured $l_A = 303 \pm 1$ and $\Omega_m h^2 = 0.13 \pm 0.01$ [29]. We assume that the *Planck* satellite will measure $\Omega_m h^2$ to a fractional error of $\sim 1\%$ and l_A to fractional error of 0.1%.

The acoustic scale is defined by $l_A = \pi D_\star / s_\star$, where $D_\star$ is the distance to the last-scattering surface at $z = 1089$. The sound horizon at decoupling, $s_\star$, is approximately given by $s_\star = 144.4\ \mathrm{Mpc}(\Omega_m h^2/0.14)^{-0.252}$ [10]. Given the dependence of these observables on the cosmological parameters $\boldsymbol{p} = \{h, \Omega_m, w\}$, we can then estimate parameter errors using the Fisher matrix:

$$F_{ij} = \frac{\partial_i l_A \partial_j l_A}{\sigma_A^2} + \frac{\partial_i \Omega_m h^2 \partial_j \Omega_m h^2}{\sigma_{\omega_m}^2} + \int_0^{z_{\max}} \frac{dN}{dz} \frac{\partial_i D_L(z) \partial_j D_L(z)}{\sigma_D(z)^2 + (\sigma_z \frac{dD_L}{dz})^2} dz, \qquad (21)$$

where redshift errors σ_z are caused by peculiar velocities[3] with assumed rms of 300 km/s. The luminosity distance $D_L(z) = (1+z)D(z)$, and its error σ_D, include both GW errors, as computed in the previous section, and gravitational lensing errors [30], computed using an approximate nonlinear power spectrum [31].

For the source redshift distribution dN/dz, we assume that short GRBs occur at a constant comoving rate of 10 $\mathrm{Gpc}^{-3}\,\mathrm{yr}^{-1}$ [32]. We found in the previous section that the SNR in distance determination per source scales roughly like $1/D$. Since the number of sources scales with volume $\propto D^3$, we expect the SNR on the Hubble constant h to scale like $D_{\max}^{1/2}$, where $D_{\max}$ is the maximum distance to

[3]It may be preferable to measure redshifts of the host galaxies rather than the GRBs themselves, whose progenitors may suffer kicks which will add in quadrature to the redshift noise from peculiar velocities.

which GRBs may be detected as gravitational-wave sources.

The standard threshold used in the GW literature for detection has been SNR >8.5 [14,33]. The reason for this high threshold is that sources are detected by correlating the data timestream with large numbers (e.g. 10^{15}) of templates corresponding to different parameter values, and therefore the detection threshold must be set high to avoid excessive numbers of false detections. Such large numbers of templates are required in order to fully explore parameter space. For GRB sources, however, the parameter space to be searched is considerably reduced: the γ-ray burst itself determines the source direction $\hat{\boldsymbol{n}}$ and time t_c. Depending upon one's confidence in theoretical models for GRBs, the chirp mass $\mathcal{M}$ and orientation $\hat{\boldsymbol{L}}$ may also constrained. Because many fewer templates need to be run for GRB sources, we should set the detection threshold correspondingly lower. We conservatively estimate that knowledge of the time of the GRB event reduces the number of required templates by a factor $\sim 10^5$, corresponding to a reduced threshold SNR >7. Note that this is the *total* SNR; since we have assumed a network of four detectors with identical noise, this translates into a threshold SNR >3.5 per detector. From this we can determine the maximum distance to which sources may be detected using Eq. (16). For chirp mass $\mathcal{M} = 1.2 M_\odot$, we have $\mathcal{A} = 4.7 \times 10^{-6}$ sec$^{5/6}$, and for our assumed noise spectral density (Fig. 1), $I_7 = 8.33 \times 10^{44}$ Hz$^{-1/3}$. Therefore the maximum distance for which $\mathrm{SNR}_{\mathrm{ave}} > 3.5$ is $D_{\mathrm{max}} = 600$ Mpc. With our assumed rate density of 10 events yr^{-1} Gpc^{-3}, we expect to measure 9 events per year out to this distance.

Assuming default cosmological parameters $h = 0.72$, $\Omega_m = 0.27$, and $w = -1$, the resulting parameter errors computed from Eq. (21) are shown in Fig. 4, as a function of the time and sky area over which GRBs are observed. While errors on the Hubble constant scale like $\sigma_h \propto N_{\mathrm{GRB}}^{-1/2}$, the errors on w scale this way only in the limit of small numbers of sources. Quite rapidly, the limiting error on w becomes the uncertainty in the CMB measurements (in the figure, fractional errors of 1% on $\Omega_m h^2$ were assumed). Unless CMB errors can be significantly improved, it will be difficult for low-redshift GW sources to constrain w to better than the few percent level.

Higher redshift standard sirens would probe departures of the cosmic expansion from linear Hubble scaling, and thereby directly constrain parameters like Ω_m and w. Unfortunately, stellar-mass inspirals at high-redshift are not sufficiently luminous to be detected by any existing or planned GW observatory. Inspirals involving SMBBH, however, are sufficiently luminous in GWs to be detected at cosmological distances. As discussed by Holz and Hughes [6], *LISA* observations of SMBBH inspirals can in principle measure distances to better than 1% accuracy. This precision is degraded, however, by gravitational lensing caused by density fluctuations from large-scale structure along the line of sight to the source. Another difficulty in using *LISA* observations is that, unlike in the case of short GRBs, for SMBBHs there are no guaranteed electromagnetic counterparts. However, it has been argued that many SMBBH mergers will be followed by bright quasar-like activity [34], or possibly preceded by optical emission [35], which will localize the GW source on the sky and provide a source redshift.

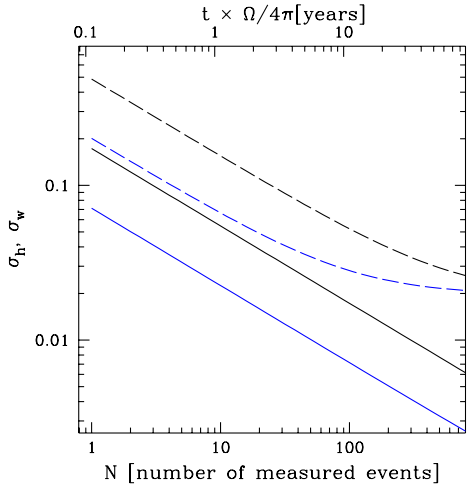

FIG. 4 (color online). Errors on h and w as a function of detected GRBs, assuming *Planck*-quality errors from CMB. Solid curves are for σ_h, the error on the Hubble constant, while dashed curves correspond to σ_w, for the dark energy equation of state parameter. The lower curves are for beamed GRBs with $\sigma_v = 0.05$, while the upper curves are for unbeamed GRBs. As discussed in the text, we assume an event rate density of 10 events per year per Gpc^{-3}; the tick marks at the top of the plot show the exposure corresponding to the detected number for the assumed rate density.

Because of lensing errors, small numbers of *LISA* sources will generally be unable to constrain dark energy parameters significantly [6]. The effects of lensing diminish significantly at lower redshifts, so a single SMBBH inspiral at $z < 0.5$ observed by *LISA* could measure the Hubble constant to $\lesssim 1\%$ and w to $\lesssim 10\%$. Although such a source is unlikely, the low-redshift regime should already be well-determined by ground-based GW observations of short GRBs. On the other hand, if large numbers of SMBBH mergers occur during *LISA*'s lifetime, then *LISA* should provide quite interesting constraints on dark energy, despite the lensing noise. To illustrate this, Fig. 5 plots expected constraints in the Ω_m vs h plane for a sample of 100 SMBBH inspirals observed by *LISA*, distributed in redshift assuming a constant comoving density between $0 < z < 2$, combined with constraints from *Planck*-quality CMB data. The 1-σ errors on w are $\sigma_w = 0.04$; these are competitive with ambitious Type-Ia supernova surveys like Joint Dark Energy Mission . Note that these errors improve

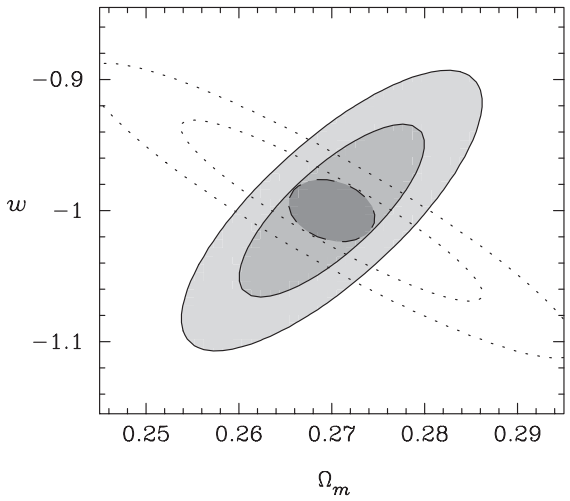

FIG. 5. *LISA* constraints on dark energy. The solid contours show the 68% and 95% confidence regions expected for a sample of 100 SMBBH sources observed by *LISA*, distributed with constant comoving density between $0 < z < 2$. A *Planck* prior has been used on $\Omega_m h^2$ and l_A, as discussed in the text. The dotted contours correspond to a sample of 3000 SNe with intrinsic luminosity scatter of 10%, with redshift distribution $\propto \exp(-(z-0.5)^2)$ over $0.02 < z < 2$. The dashed (dark shaded) contour shows the 68% confidence region for the combined constraints GW + SNe + CMB.

considerably if the main source of noise, gravitational lensing, can be cleaned out by reconstructing the lensing mass distribution using other probes. Dalal *et al.* [30] argue that cosmic shear measured from optical surveys would not allow mass reconstruction with sufficient angular resolution. Cosmic magnification measured in the radio could conceivably offer an alternative route (e.g., [36]).

Our discussion has focused on gravitational lensing only as a source of noise, but in principle there is cosmological information which can be extracted from the lensing fluctuations themselves. With large numbers of sources, *LISA* observations of cosmic magnification can provide constraints complementary to other probes. We would not expect GW standard sirens to usefully probe the power spectra of matter fluctuations or galaxy-mass correlations [9] at any scale, compared to other means like cosmic shear or Type-Ia supernovae, based on their noise power spectra :

$$\frac{\gamma_{\rm gal}^2}{n_{\rm gal}} \ll \frac{\sigma_{\rm SN}^2}{n_{\rm SN}} \ll \frac{\sigma_{\rm GW}^2}{n_{\rm GW}}, \tag{22}$$

where galaxies have shape noise $\gamma_{\rm gal} \approx 0.4$ and number density $n_{\rm gal} \approx 50/\text{arcmin}^2$, supernovae have luminosity dispersion $\sigma_{\rm SN} \approx 0.1$ and number density $n_{\rm SN} \approx 4000/(20\ \text{deg})^2$ as observed by SNAP, and GW standard sirens have luminosity errors $\sigma_{\rm GW} \approx 1\%$ and number density $n_{\rm GW} \approx 100/(4\pi\text{sr})$. On the other hand, GW standard sirens can determine 1-point functions of the matter density better than other methods, in particular, the probability distribution of lensing magnification. This could be useful for distinguishing between different dark matter models [37].

V. DISCUSSION

We have shown that observations of the GWs emitted by binary compact-object inspirals can be a powerful probe of cosmology. In particular, short γ-ray bursts appear quite promising as potential GW standard sirens. The presently observed rate of short GRBs is sufficiently high that within a few years of observation by the next generation of ground-based GW observatories (e.g. Advanced LIGO, Virgo, and AIGO), strong constraints on dark energy parameters may be derived ($\sigma_w < 0.1$). These inspiraling NS binaries should be clean sources of GWs; possible sources of contamination, such as tidal effects, magnetic torques, or gasdynamical torques from circumbinary gas, should all be negligible during the crucial inspiral phase (where $v/c \lesssim 0.3$). We emphasize that the best distance measurements come from combining multiple GW data from instruments that are widely separated. Good information about the collimation of the gamma rays, and thus on the likely inclination of the binary progenitors, will also improve the utility of these standard sirens. Given the great cosmological potential of GW observations of short GRBs, there is strong incentive to extend the lifetime of GRB satellites, such as *Swift*, to overlap with next-generation gravitational-wave observatories.

We have largely focused on the most optimistic scenario—a mature network of four advanced gravitational-wave detectors widely scattered over the globe. We have also, for ease of calculation, used the Gaussian approximation to the likelihood function in our parameter estimation. In future work we intend to simultaneously relax both of these assumptions. Indeed, as a preliminary step we have examined—in the Gaussian approximation—the effect of reducing the number of detectors in our network. We find that in going from 4 detectors to 3 (dropping the Australian detector AIGO from our network), the degradation in parameter accuracy largely scales with the degradation in total SNR *if* we impose a prior on the binary's inclination. In this case, to a good approximation, the parameter errors we have discussed throughout this paper carry through with a prefactor $\sqrt{4/3} \simeq 1.15$. It should be emphasized that the Gaussian approximation is only accurate in the "high SNR" limit; it is almost certain that we are not in this limit, and further abuse of the Gaussian approximation would simply provide spuriously optimistic estimates. In future work (currently in progress), we will examine GW-GRB siren measurements using only the LIGO detectors, the LIGO and Virgo detectors, and the four detector LIGO-Virgo-AIGO network. In doing so, we will also quantify the error induced by using the Gaussian approximation to estimate parameters in GW measurements.

The inspirals of SMBBH binaries observed by *LISA* can also provide interesting constraints on dark energy, if the rate of such mergers is high enough to average away noise caused by gravitational lensing. At present, the total rate and redshift distribution of SMBBH mergers are not well-understood, with estimates ranging from a few (or zero) per year, up to hundreds per year, depending upon assumptions [38–41]. If the rates are at the high end of these estimates, with a significant fraction at redshifts $z < 2$, then w may be constrained at the few percent level.

ACKNOWLEDGMENTS

We thank Olivier Doré, Éanna Flanagan, Wendy Freedman, Samaya Nissanke, Mike Nolta, Maria Alessandra Papa, Sterl Phinney, Roman Rafikov, and Ravi Sheth for useful discussions. David Blair, Raffaele Flaminio, and David Shoemaker provided updated coordinates and orientations for AIGO, LIGO, and Virgo. We also thank Martin Hendry and the organizers of the ETSU workshop on gravitational waves, where this work was initiated. N. D. is supported by CITA and the National Science and Engineering Research Council of Canada. D. E. H. acknowledges support from LANL, and from Willie Nelson. S. A. H. is supported by NSF grants No. PHY-0244424 and PHY-0449884, by NASA Grants No. NAG5-12906 and NNG05G105G, and by MIT's Class of 1956 Career Development Fund. B. J. is supported by NASA grant No. NAG5-10924 and by NSF grant No. AST03-07297.

[1] B. Abbott *et al.*, Phys. Rev. D **72**, 102004 (2005).
[2] B. C. Barish and R. Weiss, Phys. Today **52**, No. 10, 44 (1999).
[3] B. F. Schutz, Nature (London) **323**, 310 (1986).
[4] D. F. Chernoff and L. S. Finn, Astrophys. J. Lett. **411**, L5 (1993).
[5] L. S. Finn, Phys. Rev. D **53**, 2878 (1996).
[6] D. E. Holz and S. A. Hughes, Astrophys. J. **629**, 15 (2005).
[7] L. Blanchet, Living Rev. Relativity **5**, 3 (2002).
[8] B. Kocsis, Z. Frei, Z. Haiman, and K. Menou, Astrophys. J. **637**, 27 (2006).
[9] W. Hu and B. Jain, Phys. Rev. D **70**, 043009 (2004).
[10] W. Hu, Astron. Soc. Pac. Conf. Ser. **399**, 215 (2005).
[11] G. Bernstein, Astrophys. J. **637**, 598 (2006).
[12] L. Knox, Phys. Rev. D **73**, 023503 (2006).
[13] D. E. Holz and E. V. Linder, Astrophys. J. **631**, 678 (2005).
[14] C. Cutler and É. E. Flanagan, Phys. Rev. D **49**, 2658 (1994).
[15] L. S. Finn, Phys. Rev. D **46**, 5236 (1992).
[16] N. Gehrels, C. L. Sarazin, P. T. O'Brien, B. Zhang, L. Barbier, S. D. Barthelmy, A. Blustin, D. N. Burrows, J. Cannizzo, J. R. Cummings *et al.*, Nature (London) **437**, 851 (2005).
[17] E. Berger, P. A. Price, S. B. Cenko, A. Gal-Yam, A. M. Soderberg, M. Kasliwal, D. C. Leonard, P. B. Cameron, D. A. Frail, S. R. Kulkarni *et al.*, Nature (London) **438**, 988 (2005).
[18] D. B. Fox, D. A. Frail, P. A. Price, S. R. Kulkarni, E. Berger, T. Piran, A. M. Soderberg, S. B. Cenko, P. B. Cameron, A. Gal-Yam *et al.*, Nature (London) **437**, 845 (2005).
[19] S. D. Barthelmy, G. Chincarini, D. N. Burrows, N. Gehrels, S. Covino, A. Moretti, P. Romano, P. T. O'Brien, C. L. Sarazin, C. Kouveliotou *et al.*, Nature (London) **438**, 994 (2005).
[20] R. Narayan, B. Paczynski, and T. Piran, Astrophys. J. Lett. **395**, L83 (1992).
[21] A. I. MacFadyen, E. Ramirez-Ruiz, and W. Zhang, astro-ph/0510192.
[22] L. S. Finn, S. D. Mohanty, and J. D. Romano, Phys. Rev. D **60**, 121101 (1999).
[23] N. Seto, astro-ph/0512212.
[24] D. N. Burrows, D. Grupe, M. Capalbi, A. Panaitescu, S. K. Patel, C. Kouveliotou, B. Zhang, P. Meszaros, G. Chincarini, N. Gehrels, and R. A. M. Wijers, astro-ph/0604320.
[25] D. Grupe, D. N. Burrows, S. K. Patel, C. Kouveliotou, B. Zhang, P. Meszaros, N. Gehrels, and R. A. M. Wijers, astro-ph/0603773.
[26] E. Gustafson, D. Shoemaker, K. Strain, and R. Weiss, http://www.ligo.caltech.edu/docs/T/T990080-00.pdf (1999).
[27] F. Acernese, P. Amico, M. Al-Shourbagy, S. Aoudia, S. Avino, D. Babusci, G. Ballardin, R. Barillé, F. Barone, L. Barsotti *et al.*, Classical Quantum Gravity **22**, S869 (2005).
[28] D. E. McClelland, D. G. Blair, and R. J. Sandeman, in *Proceedings of the Seventh Marcel Grossman Meeting on Recent Developments in Theoretical and Experimental General Relativity, Gravitation, and Relativistic Field Theories* (World Scientific Press, Singapore, 1996), p. 1415.
[29] D. N. Spergel, R. Bean, O. Doré, M. R. Nolta, C. L. Bennett, G. Hinshaw, N. Jarosik, E. Komatsu, L. Page, H. V. Peiris *et al.*, astro-ph/0603449.
[30] N. Dalal, D. E. Holz, X. Chen, and J. A. Frieman, Astrophys. J. Lett. **585**, L11 (2003).
[31] R. E. Smith, J. A. Peacock, A. Jenkins, S. D. M. White, C. S. Frenk, F. R. Pearce, P. A. Thomas, G. Efstathiou, and H. M. P. Couchman, Mon. Not. R. Astron. Soc. **341**, 1311 (2003).
[32] E. Nakar, A. Gal-Yam, and D. B. Fox, astro-ph/0511254.

[33] É. É. Flanagan and S. A. Hughes, Phys. Rev. D **57**, 4535 (1998).
[34] M. Milosavljević and E. S. Phinney, Astrophys. J. Lett. **622**, L93 (2005).
[35] P. J. Armitage and P. Natarajan, Astrophys. J. Lett. **567**, L9 (2002).
[36] U.-L. Pen, New Astron. Rev. **9**, 417 (2004).
[37] U. Seljak and D. E. Holz, Astron. Astrophys. **351**, L10 (1999).
[38] A. Sesana, F. Haardt, P. Madau, and M. Volonteri, Astrophys. J. **611**, 623 (2004).
[39] K. Menou, Z. Haiman, and V. K. Narayanan, Astrophys. J. **558**, 535 (2001).
[40] M. G. Haehnelt, Classical Quantum Gravity **20**, S31 (2003).
[41] S. M. Koushiappas and A. R. Zentner, Astrophys. J. **639**, 7 (2006).